Sundberg, R. T., & Martin, R. B. (1974) *Chem. Rev. 74*, 471–517.
Swift, T. J., & Connick, R. E. (1962) *J. Chem. Phys. 37*, 307–320.
Taylor, J. S., & Coleman, J. E. (1971) *J. Biol. Chem. 246*, 7058–7067.
Terenzi, M., Rigo, A., Franconi, C., Mondovi, B., Calabrese, L., & Rotilio, G. (1974) *Biochim. Biophys. Acta 351*, 230–236.
Vänngård, T. (1972) in *Biological Applications of Electron Spin Resonance* (Swartz, H. M., Bolton, J. R., & Borg, D. C., Eds.) pp 411–447, Wiley-Interscience, New York.

Carbon-13 Nuclear Magnetic Resonance Relaxation Studies of Internal Mobility of the Polypeptide Chain in Basic Pancreatic Trypsin Inhibitor and a Selectively Reduced Analogue†

R. Richarz, K. Nagayama,‡ and K. Wüthrich*

ABSTRACT: ^{13}C nuclear spin relaxation times and ^{13}C (^1H) nuclear Overhauser effects for the backbone α carbons, the protonated aromatic ring carbons, and the side-chain methyl carbons were measured in 25 mM solutions of the basic pancreatic trypsin inhibitor and a modified analogue obtained by reduction of the disulfide bond 14–38. The relaxation parameters for the methyl carbons could, on the basis of previous individual assignments, be correlated with specific locations in the molecular structure. Analysis in terms of a "wobbling in a cone" model, where isotropic overall rotational motion of the protein was assumed, showed that, in addition to the overall rotational motions of the molecule and the rotation of the methyl groups about the C–C bond, the relaxation data manifested librational motions of the polypeptide backbone and the amino acid side chains. The following parameters for the molecular mobility resulted from this analysis: for the overall rotational motions, $\tau_R = 4 \times 10^{-9}$ s; for the librational "wobbling" of the backbone α carbons, in a cone with $\theta_{max} = 20°$, $\tau_w = 1 \times 10^{-9}$ s; for the librational motions of individual aliphatic side chains in cones with θ_{max} varying between 30° and 60°, $\tau_w = 4 \times 10^{-10}$–$3 \times 10^{-9}$ s; for methyl rotation about the C–C bond, $\tau_F \lesssim 1 \times 10^{-11}$ s. From comparison of the two proteins, the molecular motions manifested in the ^{13}C relaxation parameters were found not to be correlated with the thermal stability of the globular conformation. This coincides with the behavior of aromatic ring flips and is different from that of the exchange rates for interior amide protons, which provides new information to further characterize the previously suggested hydrophobic cluster structure for globular proteins in solution.

The small globular protein BPTI,[1] which consists of a single polypeptide chain of 58 amino acid residues and has a molecular weight of 6500, has been used extensively for studies of fundamental aspects of protein conformation. A highly refined crystal structure at 1.5-Å resolution is available (Deisenhofer & Steigemann, 1975), and high-resolution NMR studies showed that the average spatial structure in aqueous solution corresponds very closely to that seen in single crystals (Richarz & Wüthrich, 1978; Wüthrich et al., 1978; Perkins & Wüthrich, 1978, 1979; Dubs et al., 1979). ^1H NMR was further used to investigate dynamic aspects of the globular form of BPTI and related proteins. These studies have so far mainly concentrated on measurements of the internal mobility of aromatic rings (Wagner et al., 1976), exchange of internal amide protons with the solvent (Wüthrich & Wagner, 1979; Richarz et al., 1979; Wagner & Wüthrich, 1979a), and thermal denaturation (Wagner & Wüthrich, 1978; Wüthrich et al., 1979a,b), i.e., relatively infrequent stochastic events, with characteristic times of $\gtrsim 1 \times 10^{-5}$ s, which consist of concerted motions involving sizable fractions of the protein structure (Hetzel et al., 1976; Wagner & Wüthrich, 1978, 1979b; Wüthrich & Wagner, 1978; Wüthrich et al., 1979b). In contrast, NMR relaxation studies (Doddrell et al., 1972; Wüthrich, 1976), X-ray techniques (Artymiuk et al., 1979; Frauenfelder et al., 1979; Huber, 1979), and molecular dynamics calculations (McCammon et al., 1977; Karplus & McCammon, 1979) have so far, for physical or practical reasons, provided exclusively information relating to much more frequent events, in the time range 1×10^{-8}–1×10^{-12} s. The present paper describes an attempt to correlate structural information obtained from measurements on largely different time scales. It reports on comparative ^{13}C NMR relaxation studies of BPTI and a chemically modified analogue, which were previously also investigated by the above-mentioned "slow" ^1H NMR experiments.

The strategy for the present investigation was influenced by previously recorded data on the ^{13}C NMR spectra of BPTI as well as by certain practical considerations. Since the relaxation parameters were markedly affected by higher BPTI concentrations (Wüthrich & Baumann, 1976), the present

† From the Institut für Molekularbiologie und Biophysik, Eidgenössische Technische Hochschule, CH-8093 Zürich-Hönggerberg, Switzerland. *Received April 17, 1980.* This work was supported by the Swiss National Science Foundation (Project 3.0040.76).

‡ Present address: Department of Physics, University of Tokyo, Tokyo, Japan.

[1] Abbreviations used: BPTI, basic pancreatic trypsin inhibitor (Kunitz inhibitor, Trasylol, Bayer Wuppertal, Germany); RCAM-BPTI, basic pancreatic trypsin inhibitor obtained by reduction of the disulfide bond 14–38 with the cysteinyl residues protected by carboxamidomethylation; NMR, nuclear magnetic resonance; FT, Fourier transform; ppm, parts per million; Me_4Si, tetramethylsilane; TSP, 2,2,3,3-tetradeuterio-3-(trimethylsilyl)propionate; NOE, nuclear Overhauser enhancement.

0006-2960/80/0419-5189$01.00/0 © 1980 American Chemical Society

experiments were done with a 25 mM protein concentration. So far, only one chemical modification of BPTI was prepared in sufficient quantity for ^{13}C NMR studies, i.e., RCAM-BPTI which denatures at 76 °C as compared to >95 °C for native BPTI in the same solvent (Wagner et al., 1979). Previously, individual assignments were obtained for nearly all the methyl carbon resonances in BPTI (Richarz & Wüthrich, 1977; 1978). Therefore, in addition to the α carbons of the polypeptide backbone and the protonated aromatic ring carbons, the relaxation studies concentrated mainly on the methyl carbons. For an adequate description of the complex motions of the peripheral methyl groups, a "wobbling in a cone" model (Kinosita et al., 1977) was adapted for the situations encountered with BPTI, as is described under Appendix.

Materials and Methods

The basic pancreatic trypsin inhibitor (BPTI, Trasylol, Bayer Leverkusen, Germany) was obtained from the Farbenfabriken Bayer AG. RCAM-BPTI was prepared by selective reduction of the disulfide bond 14–38 with borohydride as a reducing agent and iodoacetamide as a protecting agent (Kress et al., 1968). For the ^{13}C NMR experiments, 25 mM solutions of the proteins in D_2O were prepared. Oxygen was removed by bubbling nitrogen gas through the solutions. The pD was adjusted to 4.1 by the addition of minute amounts of 1 M DCl.

^{13}C NMR measurements at 25.1 MHz were carried out on a Varian XL-100 instrument and those at 90.5 MHz on a Bruker HX-360 spectrometer. The sample temperature in the probe of the XL-100 spectrometer was measured with a thermocouple which was inserted into the sample. On the HX-360 the temperature was measured with a maximum thermometer which was inserted into the sample. In both cases, the decoupling radio frequency field was applied during the temperature measurements. The accuracy of the temperature control was ±1 °C. Sample tubes with an outer diameter of 12 and 10 mm, respectively, were used at 25.1 and 90.5 MHz.

The longitudinal relaxation times T_1 at 25.1 MHz were measured with the inversion recovery method (Vold et al., 1968; Freemann & Hill, 1969). The pulse sequence $(180°-\tau-90°-T)_n$ was used, where τ is a variable delay time and T was at least 4 times the longest T_1 to be measured. Eleven spectra were recorded with delay times τ between 11 and 600 ms. Transients (40 000 per spectrum) were accumulated with T = 1.6 s. T_1's at 90.5 MHz were measured with the saturation recovery method (Markley et al., 1971; McDonald & Leigh, 1973) by using five 90° pulse in intervals of 1 ms between two pulses to saturate the spins. Ten spectra were recorded with delay times between 40 and 2400 ms. Transients (40 000 per spectrum) were accumulated and T_1 values were evaluated with a nonlinear least-squares fitting procedure (Gerhards & Dietrich, 1976) on a Hewlett-Packard 9830 computer. The integrated areas of the signals were used for these calculations. Nuclear Overhauser enhancements were measured by comparing the integrated intensities of the ^{13}C resonances in the proton noise-decoupled spectra with and without decoupling during a period of 2.4 s prior to the data acquisition.

Results

Figure 1 shows a ^{13}C NMR inversion recovery experiment with BPTI at 25.1 MHz. Corresponding data at 90.5 MHz were obtained with the saturation recovery method. Since the mutual overlap of lines in the spectral regions of the backbone α-carbon lines and the aromatic ring carbons makes measurements of T_1's for most of the individual resonances difficult, average values of T_1 for the groups of resonances "α" and "R" (Figure 1) were evaluated. The data for the α carbons in Table I correspond to the average for the resonances between 45 and 68 ppm (Figure 1), i.e., the glycine α carbons at around 43 ppm (Wüthrich, 1976) were not considered. The line widths are the average of the widths measured for the resolved lines, and the NOE's were obtained from integration of the resonance intensities over the spectral region α (Figure 1). Essentially identical data with those for the α carbons were obtained for the protonated aromatic ring carbons of phenylalanine and tyrosine. Figure 2 shows the high-field region of partially relaxed ^{13}C NMR spectra of BPTI with the previously established individual assignements of the methyl-carbon resonances (Richarz & Wüthrich, 1978). T_1 values and NOE's for the individual methyl carbons at 25.1 and 90.5 MHz are listed in Table II.

To investigate whether the ^{13}C relaxation parameters are correlated with the thermal stability of the globular protein,

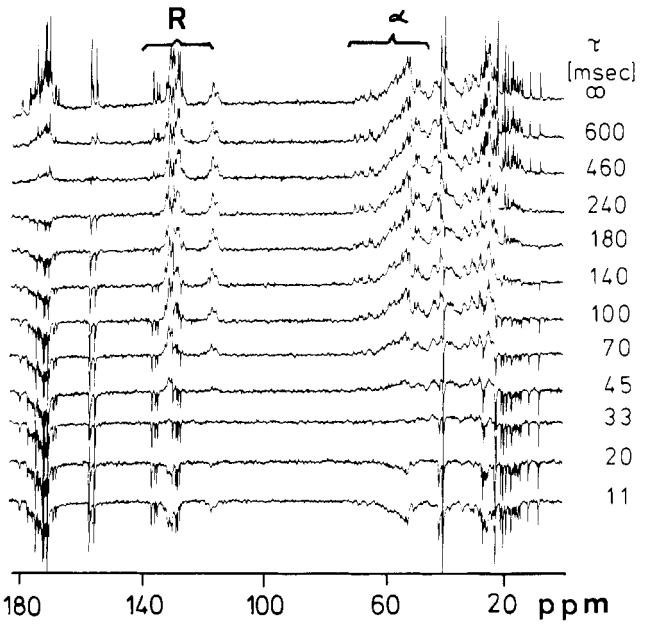

FIGURE 1: Partially relaxed proton noise-decoupled FT ^{13}C NMR spectra at 25.1 MHz of a 25 mM solution of BPTI in D_2O, at pD 4.1 and t = 39 °C. The spectra were obtained with a $(180°-\tau-90°-T)_n$ pulse sequence, with T = 1.6 s. The delay times τ are indicated on the right. The spectral regions where data for the T_1 values of the aromatic ring carbon atoms and the backbone α carbons were collected are indicated by R and α, respectively. In the R region the observed resonance intensity was corrected for the presence of the quaternary aromatic carbons.

Table I: ^{13}C NMR Relaxation Parameters for the α Carbon Resonances of BPTI[a]

resonance frequency (MHz)	parameter	exptl	calcd for best fit: isotropic rotation[c]	calcd for best fit: wobbling in a cone model[d]
25.1	T_1 (ms)	45 ± 3	40	47
	$\delta\nu_{1/2}$ (Hz)[b]	4 ± 1	5.2	4.4
	NOE	1.4 ± 0.2	1.4	1.4
90.5	T_1 (ms)	260 ± 70	210	240
	$\delta\nu_{1/2}$ (Hz)[b]	2 ± 1	3.1	2.6
	NOE	1.2 ± 0.2	1.2	1.2

[a] Measurements in a 25 mM solution of BPTI in D_2O, at pD 4.1 and t = 39 °C. [b] $\delta\nu_{1/2} = 1/(2\pi T_2)$. [c] The best fit with the assumption of isotropic rotation was obtained with $\tau_R = 3.9 \times 10^{-9}$ s. [d] The best fit with the wobbling in a cone model was obtained with the following parameters: $\tau_R = 4.0 \times 10^{-9}$ s; $\tau_W = 1.0 \times 10^{-9}$ s; $\theta_{max} = 20°$.

Table II: ^{13}C Relaxation Parameter for the Methyl-Carbon Resonances of BPTI

amino acid residue	resonance[a]	exptl and theoretical values[b]			best fit parameters[c]		
		ν_0 = 25.1 MHz		ν_0 = 90.5 MHz			
		T_1 (ms)	NOE	T_1 (ms)	τ_F (10^{-11} s)	τ_W (10^{-11} s)	θ_{max} (deg)
{Ala-16, Ala-40}	{h[d], i[d]}	160 (140)	(1.9)	260 (340)	1	100	30
Ala-25	g	155 (140)	1.9 (1.9)	320 (340)	1	100	30
Ala-27	k	150 (160)	2.3 (2.3)	210 (280)	1	300	50
Ala-48	e	150 (140)	2.0 (1.9)	310 (340)	1	100	30
Ala-58	j[d]	300 (300)	(2.5)	400 (430)	0.5	100	60
Ile-18γ	f	215 (200)	2.1 (2.3)	310 (330)	1	100	50
Ile-19γ	d	215 (230)	1.8 (2.2)	450 (410)	1	40	50
Ile-18δ	a	385 (390)	2.1 (2.3)	640 (640)	0.5	40	60
Ile-19δ	b	290 (290)	2.2 (2.0)	640 (620)	0.5	40	50
Leu-6	q	310 (290)	2.1 (2.0)	650 (620)	0.5	40	50
Met-52	c	325 (340)	2.1 (2.3)	560 (550)	0.5	70	60

[a] See Figure 2. [b] The first number in each column indicates the experimental value in a 25 mM solution of BPTI in D_2O, at pD 4.1 and t = 39 °C. The accuracy is ±15% for T_1 and ±0.2 for the NOE's. The numbers in parentheses indicate the corresponding theoretical values calculated with the wobbling in a cone model. [c] The theoretical values for T_1 and NOE were obtained as the best fits of the experimental data with the wobbling in a cone model with the parameters τ_F, τ_W, and θ_{max} given here. $\tau_R = 4 \times 10^{-9}$ s was used. [d] Because the resonances h, i, and j are mutually overlapping (Figure 2) the relaxation parameters for these lines are less accurate.

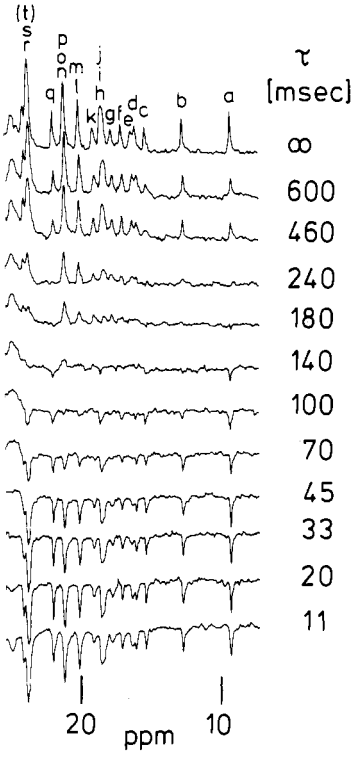

FIGURE 2: Expanded plot of the high-field region from 5 to 25 ppm of the partially relaxed ^{13}C NMR spectra of BPTI in Figure 1. The letters in the top trace indicate the previously established (Richarz & Wüthrich, 1978) assignments of the methyl-carbon lines: a and b, Ile-18δ and Ile-19δ; c, Met-52ϵ; d, Ile-19γ; e, Ala-48β; f, Ile-18γ; g, Ala-25β; (h and i), (Ala-16β and Ala-40β); j, Ala-58β; k, Ala-27β; m, Thr-11γ; n, Thr-54γ; o, Thr-32γ; q, Leu-6δ; (l, p, r, s, and t), (Leu-6δ, Leu-29δ, Leu-29δ, Val-34γ, and Val-34γ).

we compared corresponding data for BPTI and RCAM-BPTI. Previously, the denaturation temperatures at pD 5.0 were found to be >95 °C for BPTI and ~76 °C for RCAM-BPTI. Furthermore, the average spatial structures of the two proteins were found to be very similar, with local differences near the modification site in RCAM-BPTI, i.e., the reduced disulfide bond 14–38 (Wagner et al., 1979). The close similarity of the two proteins is also manifested in the ^{13}C NMR spectra. Figure 3 shows the high-field region of the spectrum of RCAM-BPTI. Comparison with Figure 2 shows that there is a 1:1 correspondence for all the methyl resonances except

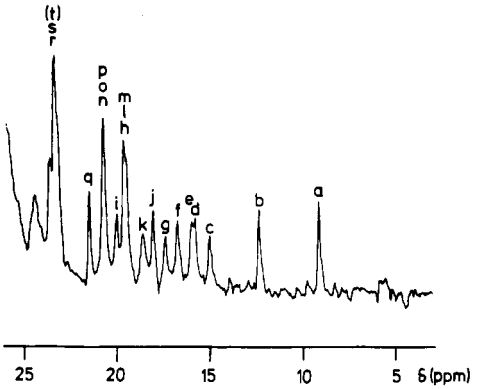

FIGURE 3: High-field region from 5 to 25 ppm of the proton noise-decoupled FT ^{13}C NMR spectrum at 25.1 MHz of a 25 mM solution of RCAM-BPTI at pD 4.1 and t = 39 °C. The letters indicate the assignments of the methyl-carbon resonances, with a 1:1 correspondence with the letters used for BPTI (see Figure 2).

Table III: Comparison of the ^{13}C Relaxation Times T_1 at 25.1 MHz in BPTI with those in RCAM-BPTI[a]

resonance[b]	assignment	T_1 (ms)	
		BPTI	RCAM-BPTI
α carbons		45 ± 3	48 ± 3
Tyr C(2,6)		46 ± 3	45 ± 5
h, i	{Ala-16β, Ala-40β}	{160 ± 20}	180 ± 30
g	Ala-25β	155	
k	Ala-27β	150 ± 20	160 ± 20
e	Ala-48β	150 ± 20	160 ± 20
j	Ala-58β	~300	300 ± 30
f	Ile-18γ	215 ± 30	170 ± 20
d	Ile-19γ	215 ± 30	200 ± 20
a	Ile-18δ	385 ± 30	360 ± 40
b	Ile-19δ	290 ± 30	240 ± 30
q	Leu-6δ	310 ± 30	210 ± 40
c	Met-25ϵ	325 ± 30	330 ± 30

[a] The relaxation times were measured in 25 mM solutions of the proteins in D_2O, at pD 4.1 and t = 39 °C. [b] See Figures 2 and 3.

h and i, which have slightly different chemical shifts in the two proteins. Therefore the resonance assignments in Figure 3 were made analogous to those for BPTI. The two lines h and i were assigned to Ala-16 and Ala-40 which are immediately adjacent to the modification site. Values for the re-

laxation times T_1 for corresponding lines in the two proteins are listed in Table III.

Discussion

Overall Rotational Motions of BPTI. We adopt the generally used working hypothesis (Allerhand et al., 1971; Wilbur et al., 1976) that the relaxation parameters of the backbone α carbons are the most reliable manifestation of the overall rotational motions of a protein. With the simplifying assumptions that the rotational motions of the backbone atoms are strictly limited to the overall tumbling of the molecule and that the latter can be characterized by a single correlation time for isotropic rotational tumbling, τ_R, the experimental data of Table I correspond to $\tau_R = 3.9 \times 10^{-9}$ s. The experimental value of τ_R is thus 2–3 times longer than that estimated with the Stokes–Einstein relation (Abragam, 1962) for a spherical protein with the molecular weight of BPTI and with a hydration shell of a thickness of 2.5 Å in aqueous solution.

That the rotational correlation time is rather long, a phenomenon which was also reported from ^{13}C NMR studies of different proteins (Visscher & Gurd, 1974; Wilbur et al., 1976), appears to be primarily due to the high protein concentration. Support for this explanation comes from the observation that τ_R for BPTI in a 50 mM solution is considerably longer yet, i.e., 2×10^{-8} s (Wüthrich & Baumann, 1976). Part of the effect of high protein concentration can be directly assessed from the increased macroscopic viscosity, which is $\sim$1.5 times that of pure D_2O in a 25 mM BPTI solution. As to other potential sources for the long τ_R, numerical calculations for an ellipsoidal shape of BPTI showed that the deviations of the molecular shape from a sphere should cause only a small increase of the effective τ_R, and, as is further discussed below, a more realistic protein model including internal segmental mobility yields nearly the same value for τ_R as the simple solid sphere approximation (Table I).

Analysis of Internal Motions by the Wobbling in a Cone Model. From basic principles it is obvious that in a protein molecule at ambient temperature all the atoms undergo intermolecular motions. In a mechanical description of the protein, one calculates a very large number of normal-mode vibrations to be assigned to bending or stretching of the individual covalent bonds. These coherent motions with frequencies $\gtrsim 1 \times 10^{12}$ s^{-1}, which are in principle accessible to observation by optical methods, are not noticeably manifested in the NMR relaxation. However, superimposed on these "elemental" thermal motions, there are further the relatively large time variations of dihedral angles about single bonds. Dampening of these rotational motions by the environment of the individual atoms in the hydrated protein structure leads to stochastic fluctuations of the peptide backbone and the amino acid side chains which may have frequency components in the range where the NMR spin relaxation can be affected.

Quite generally the rotational motions of a peptide fragment relative to the laboratory frame, which result from the combination of the overall rotation of the molecule and intramolecular motions, are very complex. Compromising between a realistic description of these complex movements and the requirement for a tractable mathematical model, we have chosen to analyze the relaxation data of BPTI in terms of a wobbling in a cone description (Kinosita et al., 1977) for stochastic internal motions. A detailed presentation of this model is given under Appendix. It can be seen that through a fit to the wobbling in a cone model the experimental relaxation parameters can be correlated with a combination of quite straightforward internal motions, such as rotation about single bonds and diffusion of a rotation axis inside a cone. In the following this treatment will be applied to different types of carbon atoms in BPTI.

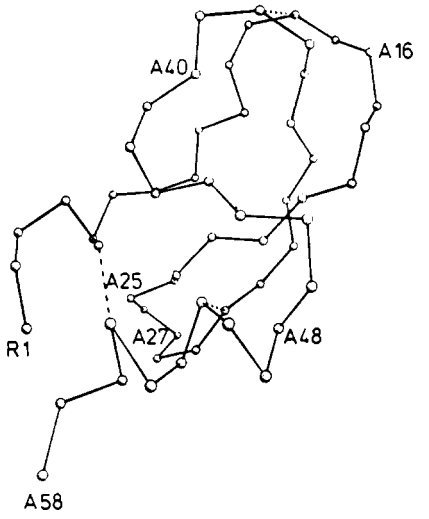

FIGURE 4: Computer drawing of the α-carbon positions in the crystal structure of BPTI (Deisenhofer & Steigemann, 1975). The locations of the three disulfide bonds 5–55, 14–38, and 30–51 are indicated by the broken lines, and the six alanines and the N terminus are identified by the IUB–IUPAC one-letter symbols and the position in the amino acid sequence.

Segmental Mobility of the Polypeptide Backbone. In a simplified form described under Appendix the wobbling in a cone model was used to analyze the relaxation parameters for the α-carbon atoms. While with the values for τ_R, τ_w, and θ_{max} given in Table I a somewhat better fit of the experimental data was obtained than with the rigid sphere approximation, the differences are too small to provide convincing evidence for backbone mobility.

More direct evidence for intramolecular motions of backbone fragments came from the data on the methyl carbons of the six alanines in BPTI. In a rigid molecular structure the internal mobility of the alanine methyl groups would be restricted to rotation about the C^α–C^β bond. This limiting situation was investigated by Woessner (1962) who showed that T_1 for the methyl carbon could be at most 3 times longer than that for the α-carbon atom. Since at 25.1 MHz the T_1's for the methyl carbons are consistently longer than this limiting value (Tables I and II), additional mobility besides methyl rotation had to be considered. Fitting the data with the wobbling in a cone model indicated that the C^α–C^β methyl rotation axes of Ala-16, -25, -40, and -48 undergo angular displacements on the order of 30° with a correlation time of $\sim 1 \times 10^{-9}$ s (Table II). A somewhat larger mobility is indicated for the backbone region near Ala-27, and the increased flexibility at the C-terminal Ala-58 is very clearly manifested.

It is interesting that the increased mobility of the polypeptide fragments near Ala-27 and near the C-terminal Ala-58 manifested in the ^{13}C NMR parameters coincides with predictions from molecular dynamics calculations on the BPTI structure (McCammon et al., 1977; Karplus & McCammon, 1979). These authors found that overall the time average of the structure of BPTI over a period of 1×10^{-10} s coincided closely with the crystal structure (Deisenhofer & Steigemann, 1975) yet that relatively large deviations were found for the polypeptide fragment 25–28, which links the two strands of the antiparallel β sheet (Figure 4), and for the two chain terminal fragments (Karplus & McCammon, 1979).

Internal Mobility of Amino Acid Side Chains. The internal mobility of the aromatic rings of phenylalanine and tyrosine in BPTI was previously investigated by ^1H NMR (Wagner

et al., 1976). Precise information was obtained for five of the eight rings. For the remaining three rings the frequency of 180° flips about the C^{β}–C^{γ} bond (Hetzel et al., 1976) was rapid on the ^1H NMR time scale, and only an upper limit for the correlation time of the internal motions could be estimated, i.e., $\tau_{180°} < 2 \times 10^{-5}$ s. The present ^{13}C relaxation study showed an essentially identical behavior for the backbone α carbons and the protonated ring carbons of the aromatics (Figure 1 and Table III). From this it can be concluded, in agreement with a previous study (Wüthrich & Baumann, 1976), that the frequency of aromatic ring flips is small compared to the overall rotation of BPTI, i.e., $\tau_{180°} > 4 \times 10^{-9}$ s. Otherwise, the relaxation data would be compatible with small-amplitude librational motions of the aromatic rings on a time scale comparable to or faster than τ_R.

For the mobility of aliphatic side chains information was obtained from analysis of the methyl-carbon relaxation parameters with the wobbling in a cone model (Table II). There is a readily apparent trend to increased mobility for the peripheral carbons in longer side chains, which is manifested in both the increased frequency of the motions and the larger half-angle θ_{max} of the cone covered by the wobbling motions. This confirms earlier conclusions which were obtained without individually assigned ^{13}C NMR data on a variety of proteins [for a survey, see Allerhand (1979)].

Internal Mobility and Stability of Globular Protein Structure. Previously, ^1H NMR studies of a group of chemically modified analogues of BPTI were used to investigate correlations between internal mobility manifested in the amide proton exchange rates (Richarz et al., 1979) and the rotational flipping motions of the aromatic rings (Wagner et al., 1976) with the thermal stability of the globular form of the proteins. While the amide proton exchange rates were found to increase when the stability of the protein was lowered, the mobility of the aromatic rings was not affected (Wagner & Wüthrich, 1978). From these observations we have suggested a hydrophobic cluster architecture which might be found not only in BPTI but also quite generally in globular proteins (Wüthrich & Wagner, 1978; Wüthrich et al., 1979a; Wagner & Wüthrich, 1979b; Wüthrich et al., 1980). It was now interesting to see how the higher frequency internal motions manifested in the ^{13}C relaxation data were affected by different thermal stabilities of two otherwise nearly identical spatial protein structures.

Table III shows that nearly identical relaxation data were obtained for corresponding resonances in BPTI and RCAM-BPTI, which have denaturation temperatures of >95 °C and ~76 °C, respectively, under the conditions used for the ^{13}C NMR studies (Wagner et al., 1979). This holds for the backbone α carbons, the aromatic ring carbons, and the methyl carbons of aliphatic side chains, with the exception of Leu-6 δCH_3 where there is evidence for reduced mobility in RCAM-BPTI. There is also some indication that the mobility of the δ methyls of Ile-18 and Ile-19 might be somewhat more restricted in RCAM-BPTI. Overall, the observations for the ^{13}C relaxation parameters are thus very similar to those for the mobility of the aromatic rings, i.e., no global effect on the relaxation times for carbon atoms located in different regions of the molecule results from a localized modification of the covalent protein structure, such as the reduction of the covalent protein structure, such as the reduction of the disulfide bond 14–38 in RCAM-BPTI (Figure 4). This appears to further substantiate the hypothesis of a hydrophobic cluster architecture of globular proteins. The aliphatic side chains form an important part of the hydrophobic clusters surrounding the aromatic rings (Wüthrich et al., 1980). That their behavior in the two proteins with different stability parallels that seen previously for the aromatic rings supports that observation of the latter provides a reliable NMR probe for studies of internal fluctuations within these clusters.

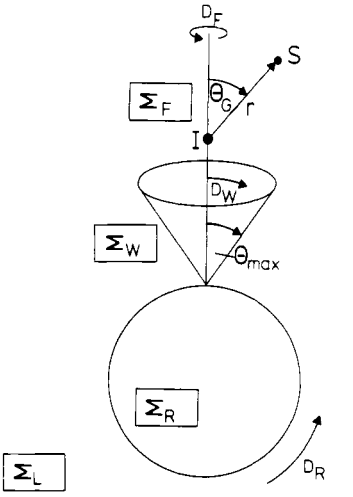

FIGURE 5: Wobbling in a cone model. We consider the relaxation of spin I by dipole–dipole coupling with spin S. The two spins are located in a spherical particle which undergoes isotropic rotational motions with a diffusion constant D_R relative to the laboratory frame $\sum_L$. The vector r which connects the two spins is attached at a fixed angle θ_G to an axis about which it rotates with a diffusion constant D_F. This rotation axis is further allowed to wobble, relative to the a coordinate system $\sum_R$ fixed in the rotating molecule, with D_W inside a cone defined by the half-angle θ_{max}. For characterization of the resulting complex motion in space of the vector r, the two coordinate systems $\sum_W$ and $\sum_F$ are used in addition to $\sum_L$ and $\sum_R$. $\sum_W$ is fixed with respect to the wobbling motion of the rotation axis inside the cone defined in the frame $\sum_R$. $\sum_F$ is fixed with respect to the rotations about this axis.

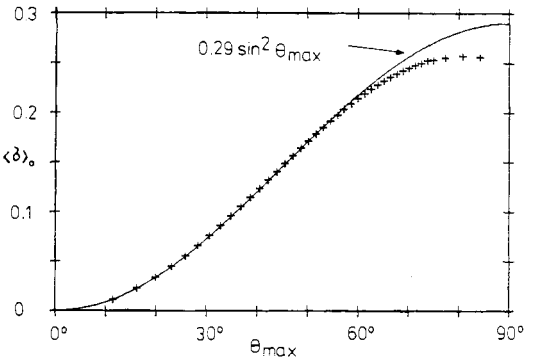

FIGURE 6: Wobbling in a cone model. Plot of $\langle\sigma\rangle_0$ vs. θ_{max}. The crosses represent the values calculated by Kinosita et al. (1977; personal communication), and the solid line represents the corresponding data obtained with the approximation $\langle\sigma\rangle_0 = 0.29 \sin^2 \theta_{max}$ (see text).

Outlook for Future Investigations. The wobbling in a cone model presents a quite realistic and tractable description of the complex intramolecular motions in a flexible protein structure (Karplus & McCammon, 1979; Wüthrich & Wagner, 1978). Overall, mainly as a result of the individual assignments for numerous ^{13}C NMR lines in BPTI (Richarz & Wüthrich, 1978), the data presented in this paper clearly provide evidence for wobbling-motion contributions to the relaxation parameters. In some instances, however, the manifestations of internal mobility were just barely discernible within the accuracy of the relaxation data. For future work it will therefore be highly desirable that more accurate relaxation parameters can be obtained. The use of the wobbling in a cone model should then also be suitable for a more

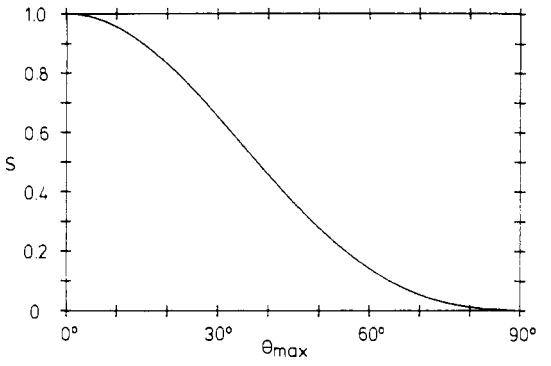

FIGURE 7: Wobbling in a cone model. Plot of S vs. θ_{max} (eq 14).

quantitative assessment of molecular regions with variable internal flexibility.

Acknowledgments

We thank Dr. R. Schmidt-Kastner, Farbenfabriken Bayer AG, for a generous gift of BPTI (Trasylol) and H. Roder for the preparation of the large amount of RCAM-BPTI needed for the ^{13}C NMR experiments. We are grateful to Dr. K. Kinosita for sending us his numerical results for the diffusion in a cone.

Appendix

The "Wobbling in a Cone" Model. Equations 1–3 describe the ^{13}C relaxation times T_1 and T_2 and the steady-state NOE which arise from dipole–dipole coupling between the observed ^{13}C nucleus and a single proton as functions of the spectral densities $J(\omega)$ (Abragam, 1962). γ_H and γ_C are the gyro-

$$T_1^{-1} = (1/3)\hbar^2\gamma_H^2\gamma_C^2 r^{-6}[J(\omega_C - \omega_H) + 3J(\omega_C) + 6J(\omega_C + \omega_H)] \quad (1)$$

$$T_2^{-1} = (1/6)\hbar^2\gamma_H^2\gamma_C^2 r^{-6}[4J(0) + J(\omega_C - \omega_H) + 3J(\omega_C) + 6J(\omega_H) + 6J(\omega_C + \omega_H)] \quad (2)$$

$$NOE = 1 + \frac{\gamma_H[6J(\omega_C + \omega_H) - J(\omega_C - \omega_H)]}{\gamma_C[J(\omega_C - \omega_H) + 3J(\omega_C) + 6J(\omega_C + \omega_H)]} \quad (3)$$

magnetic ratios for ^1H and ^{13}C, $\hbar$ is the Planck constant divided by 2π, r is the distance between the two nuclei, and ω_H and ω_C are the Larmor frequencies for ^1H and ^{13}C. The spectral densities $J(\omega)$ are the Fourier transforms of the autocorrelation functions $G(t)$

$$J(\omega) = F[G(t)] \quad (4)$$

For dipole–dipole coupling, $G(t)$ has the form

$$G^{(m)}(t) = 5\langle Y_{2m}[\Omega_{L\to F}(0)]Y_{2m}^*[\Omega_{L\to F}(t)]\rangle \quad (5)$$

where m is the magnetic quantum number, Y_{2m} are spherical harmonics of the second rank, and $\Omega_{L\to F}$ represents the Euler transformation between the laboratory and the final coordinate system (Figure 5). In the following a wobbling in a cone model is used for the description of the movements in space of the vector $\boldsymbol{r}$ linking ^1H and ^{13}C (Figure 5). The autocorrelation functions resulting from this type of spatial motion were computed with the formalism of Wallach (1967). In eq 6 the transformation between the laboratory system and the rotating coordinate system Σ_F (Figure 5) is separated into a series of steps, where the Euler angles α, β, and γ are used as arguments. In the derivation of eq 6 it was further assumed that the three types of diffusional motion characterized by the diffusion constants D_R, D_W, and D_F (Figure 5) are not correlated and that the angle θ_G is fixed. The functions

$$G^{(m)}(t) = 5\sum_{a,b}\langle D_{ma}^{(2)}(\alpha_{L\to R},\beta_{L\to R},\gamma_{L\to R};0)D_{ma}^{(2)*} \times (\alpha_{L\to R},\beta_{L\to R},\gamma_{L\to R};t))\langle D_{ab}^{(2)}(\alpha_{R\to W},\beta_{R\to W},\gamma_{R\to W};0) \times D_{ab}^{(2)*}(\alpha_{R\to W},\beta_{R\to W},\gamma_{R\to W};t)\rangle|Y_{2b}(\beta_{W\to F};0)|^2 = \sum_{b=-2}^{2}\exp(6D_R t)|Y_{2b}(\beta_{W\to F};0)|^2\sum_{a=-2}^{2}\langle D_{ab}^{(2)} \times (\alpha_{R\to W},\beta_{R\to W},\gamma_{R\to W};0)D_{ab}^{(2)*}(\alpha_{R\to W},\beta_{R\to W},\gamma_{R\to W};t)\rangle \quad (6)$$

$D_{mm'}^{(2)}(\alpha,\beta,\gamma)$ are elements of the Wigner rotation matrix (Wigner, 1959). For evaluation of the statistical average of the autocorrelation functions in eq 6, a Green's function for diffusion of a rigid body is generally required. The Green's function for diffusion of a unit vector in a cone was previously evaluated with the use of generalized Legendre functions $P_\nu^m(x)$, where ν takes noninteger values and m is an integer (Carslow & Jaeger, 1959). On the same theoretical basis Kinosita et al. (1977) calculated the correlation functions for the case $b = 0$. They found that the relaxation trend can be well approximated with the use of one average correlation time, while in reality the correlation function should be described by an infinite number of relaxation times. In analogy to the case $b = 0$, we used this result for the cases $b = 1$ and 2. Finally the sum of correlation functions in eq 6 is rewritten in the form

$$\sum_{a=-2}^{2}\langle D_{ab}^{(2)}(\alpha_{R\to W},\beta_{R\to W},\gamma_{R\to W};0)D_{ab}^{(2)*} \times (\alpha_{R\to W},\beta_{R\to W},\gamma_{R\to W};t))\rangle \cong [S_b + (1 - S_b)\exp(-D_W t\langle\sigma\rangle^{-1})]\exp[-b^2(D_F - D_W)t] \quad (7)$$

where

$$S_b = (1/4)\cos^2\theta_{max}(1 + \cos\theta_{max})^2 \text{ for } b = 0 \quad (8a)$$

and

$$S_b = 0 \text{ for } b \neq 0 \quad (8b)$$

and where three individual correlation times are defined by

$$\tau_R = \frac{1}{6D_R} \qquad \tau_W = \frac{1}{D_W} \qquad \tau_F = \frac{1}{D_F} \quad (9)$$

The correlation time for diffusional wobbling in the cone was found to be defined by eq 10. In eq 10 $d_{ab}^{(2)}(\beta) = D_{ab}^{(2)}(0,\beta,0)$

$$\tau_W\langle\sigma\rangle_b(1 - S_b) = \sum_{a=-2}^{2}\int_0^\infty dt\int_0^{\theta_{max}}\int_0^{\theta_{max}}[d_{ab}^{(2)}(\beta)d_{ab}^{(2)}(\beta')p(\beta,\beta',t)p_0] \, d(\cos\beta)\, d(\cos\beta') \quad (10)$$

is an element of the reduced Wigner rotation matrix (Wigner, 1959). The running variable in the integration, β, corresponds to $\beta_{R\to W}$ in eq 6 and 7. θ_{max} is defined in Figure 5. p_0 is the initial distribution, and $p(\beta,\beta',t)$ is the transition probability for the time evolution of β which obeys diffusion eq 11 subject

$$-\frac{\partial}{\partial t}p(\beta,\beta',t) = D_W\left[\frac{\partial}{\partial\beta^2} + \cot\beta\frac{\partial}{\partial\beta} - \frac{1}{\sin^2\beta}(a^2 + b^2 - 2ab\cos\beta)\right]p(\beta,\beta',t) \quad (11)$$

to the initial condition $p(\beta,\beta',0) = \delta(\beta - \beta')$ and the boundary condition $(\partial p/\partial\beta)|_{\beta=\theta_{max}} = 0$. For the case $b = 0$, the summation in eq 10 is over all values of $|a| \leq 2$ except $a = 0$. From eq 10 one sees immediately that the average correlation time $\tau_W\langle\sigma\rangle_b$ depends on the angle θ_{max} even if one assumes that the diffusional wobbling in the cone can be described by a single diffusion constant, D_W.

The numerical calculation of $\langle\sigma\rangle_0$ has been first performed by Kinosita et al. (1977), and an analytical solution was recently proposed by Lipari & Szabo (1980). We find that in the range $0° < \theta_{max} < 70°$ it is well approximated within an error of 5% (see Figure 6) by the simple expression

$$\langle\sigma\rangle_0 = 0.29 \sin^2 \theta_{max} \quad (12)$$

The general expression for the spectral density is

$$J(\omega) = A\left[S\frac{\tau_A}{1+(\tau_A\omega)^2} + (1-S)\frac{\tau_A'}{1+(\tau_A'\omega)^2}\right] + B\frac{\tau_B}{1+(\tau_B\omega)^2} + C\frac{\tau_C}{1+(\tau_C\omega)^2} \quad (13)$$

with

$$\tau_A^{-1} = \tau_R^{-1}$$
$$\tau_A'^{-1} = \tau_R^{-1} + \tau_W^{-1}\langle\sigma\rangle_0^{-1}$$
$$\tau_B^{-1} = \tau_R^{-1} + (1/6)\tau_F^{-1} + \tau_W^{-1}(\langle\sigma\rangle_1^{-1} - 1)$$
$$\tau_C^{-1} = \tau_R^{-1} + (2/3)\tau_F^{-1} + \tau_W^{-1}(\langle\sigma\rangle_2^{-1} - 4)$$
$$S = (1/4)\cos^2\theta_{max}(1+\cos\theta_{max})^2 \quad (14)$$
$$A = (1/4)(3\cos^2\theta_G - 1)^2$$
$$B = 3\sin^2\theta_G\cos^2\theta_G$$
$$C = (3/4)\sin^4\theta_G$$
$$\langle\sigma\rangle_0 = 0.29\sin^2\theta_{max} \quad (0° \le \theta_{max} \le 70°)$$

(See Figure 7.) For the situations of special interest in the present investigation, the terms in $\langle\sigma\rangle_1$ and $\langle\sigma\rangle_2$ vanish (see below). Hence these terms have not as yet been calculated.

Treatment of Relaxation of α Carbon in a Protein with the Wobbling in a Cone Model. The general case treated so far included wobbling of an axis in a cone combined with rotation about this axis (Figure 5). For the motion of the vector between an α carbon and the directly attached proton, no rotation about the wobbling axis must be considered. This case may be described by assuming that either $\theta_G = 0$ or $D_F = 0$ in eq 13 and 14, which leads to the expression for the spectral density

$$J(\omega) = S\frac{\tau_A}{1+(\tau_A\omega)^2} + (1-S)\frac{\tau_A'}{1+(\tau_A'\omega)^2} \quad (15)$$

where

$$\tau_A^{-1} = \tau_R^{-1}$$
$$\tau_A'^{-1} = \tau_R^{-1} + \tau_W^{-1}\langle\sigma\rangle_0^{-1}$$
$$S = (1/4)\cos^2\theta_{max}(1+\cos\theta_{max})^2$$
$$\langle\sigma\rangle_0 = 0.29\sin^2\theta_{max} \quad (0° \le \theta_{max} \le 70°)$$

Inserting eq 15 into eq 1–3 gives the final result for the relaxation times and the NOE of the α carbons in a protein for the situation where the flexibility of the backbone is described by a wobbling in a cone motion. Note that the well-known result for isotropic rotational motion is obtained either for $\tau_W \to \infty$ or for $\theta_{max} \to 0$.

Treatment of Relaxation of Methyl Carbons in a Protein with the Wobbling in a Cone Model. Here, the rotation of the methyl group about the C–C bond must be considered in addition to the wobble of the rotation axis (Figure 5). With the realistic assumption that the rotation of the methyl group described by τ_F is rapid compared to the wobbling rate, τ_B and τ_C in eq 13 and 14 can be reduced to

$$\tau_B^{-1} = \tau_R^{-1} + (1/6)\tau_F^{-1}$$
$$\tau_C^{-1} = \tau_R^{-1} + (2/3)\tau_F^{-1} \quad (16)$$

for $\tau_F \ll \tau_W$. Note that one obtains the well-known formulas of Woessner (1962) for a rapidly rotating methyl group rigidly attached to a sphere when $\tau_W \to \infty$ or $\theta_{max} \to 0$.

References

Abragam, A. (1962) *The Principles of Nuclear Magnetism*, Clarendon Press, Oxford.

Allerhand, A. (1979) *Methods Enzymol. 61*, 458.

Allerhand, A., Doddrell, D., Glushko, V., Cochran, D. W., Wenkert, E., Lawson, P. J., & Gurd, F. R. N. (1971) *J. Am. Chem. Soc. 93*, 544.

Artymink, P. J., Blake, C. C. F., Grace, D. E. P., Oatley, S. J., Phillips, D. C., & Sternberg, M. J. E. (1979) *Nature (London) 280*, 563.

Carslaw, H. S., & Jaeger, J. C. (1959) *Conduction of Heat in Solids*, 2nd ed., Chapter 14, Clarendon Press, Oxford.

Deisenhofer, J., & Steigemann, W. (1975) *Acta Crystallogr., Sect. B 31*, 238.

Doddrell, D., Glushko, V., & Allerhand, A. (1972) *J. Chem. Phys. 56*, 3683.

Dubs, A., Wagner, G., & Wüthrich, K. (1979) *Biochim. Biophys. Acta 577*, 177.

Frauenfelder, H., Petsko, G. A., & Tsernoglou, D. (1979) *Nature (London) 280*, 558.

Freeman, R., & Hill, H. D. W. (1969) *J. Chem. Phys. 51*, 3140.

Gerhards, R., & Dietrich, W. (1976) *J. Magn. Reson. 23*, 21.

Hetzel, R., Wüthrich, K., Deisenhofer, J., & Huber, R. (1976) *Biophys. Struct. Mech. 2*, 159.

Huber, R. (1979) *Trends Biochem. Sci. (Pers. Ed.) 4*, 271.

Karplus, M., & McCammon, J. A. (1979) *Nature (London) 277*, 578.

Kinosita, K., Jr., Kawato, S., & Ikegami, A. (1977) *Biophys. J. 20*, 289.

Kress, L. F., Wilson, K. A., & Laskowski, M., Sr. (1968) *J. Biol. Chem. 243*, 1758.

Lipari, G., & Szabo, A. (1980) *Biophys. J.* (in press).

Markley, J. L., Horsley, W. J., & Klein, M. P. (1971) *J. Chem. Phys. 55*, 3604.

McCammon, J. A., Gelin, B. R., & Karplus, M. (1977) *Nature (London) 267*, 585.

McDonald, G. G., & Leigh, J. S. (1973) *J. Magn. Reson. 9*, 358.

Perkins, S. J., & Wüthrich, K. (1978) *Biochim. Biophys. Acta 536*, 406.

Perkins, S. J., & Wüthrich, K. (1979) *Biochim. Biophys. Acta 576*, 409.

Richarz, R., & Wüthrich, K. (1977) *FEBS Lett. 79*, 64.

Richarz, R., & Wüthrich, K. (1978) *Biochemistry 17*, 2263.

Richarz, R., Sehr, P., Wagner, G., & Wüthrich, K. (1979) *J. Mol. Biol. 130*, 19.

Visscher, R. B., & Gurd, F. R. N. (1975) *J. Biol. Chem. 250*, 2238.

Vold, R. L., Waugh, J. S., Klein, M. P., & Phelps, D. E. (1968) *J. Chem. Phys. 48*, 3831.

Wagner, G., & Wüthrich, K. (1978) *Nature (London) 275*, 247.

Wagner, G., & Wüthrich, K. (1979a) *J. Mol. Biol. 130*, 31.

Wagner, G., & Wüthrich, K. (1979b) *J. Mol. Biol. 134*, 75.

Wagner, G., DeMarco, A., & Wüthrich, K. (1976) *Biophys. Struct. Mech. 2*, 139.

Wagner, G., Tschesche, H., & Wüthrich, K. (1979) *Eur. J. Biochem. 95*, 239.
Wallach, D. (1967) *J. Chem. Phys. 47*, 5258.
Wigner, E. P. (1959) *Group Theory and Its Application to the Quantum Mechanics of Atomic Spectra*, Academic Press, New York.
Wilbur, D. J., Norton, R. S., Clouse, A. O., Addleman, R., & Allerhand, A. (1976) *J. Am. Chem. Soc. 98*, 8250.
Woessner, (1962) *J. Chem. Phys. 36*, 1.
Wüthrich, K. (1976) *NMR in Biological Research: Peptides and Proteins*, North-Holland Publishing Co., Amsterdam.
Wüthrich, K., & Baumann, R. (1976) *Org. Magn. Reson. 8*, 532.
Wüthrich, K., & Wagner, G. (1978) *Trends Biochem. Sci. (Pers. Ed.) 3*, 227.
Wüthrich, K., & Wagner, G. (1979) *J. Mol. Biol. 130*, 1.
Wüthrich, K., Wagner, G., Richarz, R., & Perkins, S. J. (1978) *Biochemistry 17*, 2253.
Wüthrich, K., Roder, H., & Wagner, G. (1979a) in *Protein Folding* (Balaban, A., & Jaenicke, R., Eds.) North-Holland Publishing Co. (in press).
Wüthrich, K., Wagner, G., & Richarz, R. (1979b) *Proc. FEBS Meet. 52*, 143.
Wüthrich, K., Wagner, G., Richarz, R., & Braun, W. (1980) *Biophys. J.* (in press).

Proton Nuclear Magnetic Resonance Studies of Hemoglobins M Boston (α58E7 His → Tyr) and M Milwaukee (β67E11 Val → Glu): Spectral Assignments of Hyperfine-Shifted Proton Resonances and of Proximal Histidine (E7) NH Resonances to the α and β Chains of Normal Human Adult Hemoglobin†

Seizo Takahashi,‡ Allison K.-L. C. Lin, and Chien Ho*

ABSTRACT: High-resolution proton nuclear magnetic resonance spectroscopy at 250 MHz has been used to investigate both the ferrous and ferric hyperfine-shifted resonances of naturally occurring valency hybrid hemoglobins, Hb M Boston (α58E7 His → Tyr) and Hb M Milwaukee (β67E11 Val → Glu), in order to make a definite assignment of these resonances to the α and β chains of normal human adult hemoglobin. In Hb M Boston ($\alpha_2^+\beta_2$), the iron atoms of the α chains are in the ferric state, while those in the β chains are in the ferrous state. On the other hand, the iron atoms of the β chains in Hb M Milwaukee ($\alpha_2\beta_2^+$) are in the ferric state, while those in the α chains are in the ferrous state. Due to the difference in the number of unpaired electrons, ferric and ferrous hyperfine-shifted proton resonances occur in different regions of the spectrum. The spectrum derived from the arithmetical sum of the ferrous hyperfine-shifted proton resonances of deoxy-Hb M Boston and Hb M Milwaukee in D_2O, which appear between 6 and 18 ppm downfield from residual HDO, is found to be essentially identical with that of normal human adult deoxyhemoglobin. Thus, the assignment of the ferrous hyperfine-shifted proton resonances in this spectral region to the α and β chains of normal human adult deoxyhemoglobin has been accomplished. By means of the spectral comparison of these three hemoglobins in the deoxy form, an assignment of the proximal histidine (E7) exchangeable NH resonances to the α and β chains of normal human adult deoxyhemoglobin has also been established. These resonances are found respectively at 58.5 and 71.0 ppm downfield from H_2O. Because of the similarity of the chemical shifts of ferrous hyperfine-shifted proton resonances, it is concluded that the ferrous heme environments of unligated Hb M Boston and Hb M Milwaukee are similar to those of normal human adult deoxyhemoglobin. On the other hand, the ferric hyperfine-shifted proton resonances of Hb M Boston and Hb M Milwaukee are found to be different from those of normal human adult methemoglobin. The results suggest that the detailed environments of the ferric hemes in these hemoglobins are different.

The proton nuclear magnetic resonance (NMR)[1] spectra of hemoglobin (Hb) in the deoxy and met forms show several characteristic resonances which are remote from the majority of diamagnetic resonances. They arise from the hyperfine interactions between the unpaired electrons of the iron atoms and the proton groups on the hemes and/or the nearby amino acid residues of the α and β chains. There are two types of hyperfine-shifted resonances, Fermi contact and pseudocontact shifted resonances. [For a recent discussion on hyperfine-shifted proton resonances in heme proteins, see Ho et al. (1978) and the references cited therein.] These resonances are sensitive to the conformation of the heme groups and to the electronic spin state of the iron atoms (Kurland et al., 1968; Lindstrom et al., 1972; Ho et al., 1973, 1978; Fung et al., 1976, 1977; Viggiano & Ho, 1979; Viggiano et al., 1979). A number

† From the Department of Biological Sciences, Mellon College of Science, Carnegie-Mellon University, Pittsburgh, Pennsylvania 15213. *Received May 12, 1980.* Supported by research grants from the National Institutes of Health (HL-24525) and the National Science Foundation (PCM 78-25818). The NMR Facility in Pittsburgh is supported by a research grant from the National Institutes of Health (RR-00292). Part of this paper was presented at the Annual Meeting of the Biophysical Society, Atlanta, GA, Feb 25–28, 1979, and the Symposium on the Interaction between Iron and Proteins in Oxygen and Electron Transport, Airlie House, Airlie, VA, April 13–18, 1980.

‡ Present address: Department of Biophysics and Biochemistry, University of Tokyo, Tokyo, Japan.

[1] Abbreviations used: NMR, nuclear magnetic resonance; Hb, hemoglobin; Hb A, normal human adult hemoglobin; met-Hb, methemoglobin; Bis-Tris, [bis(2-hydroxyethyl)imino]tris(hydroxymethyl)-methane; pH*, the pH value in D_2O taken directly from the pH meter reading.

0006-2960/80/0419-5196$01.00/0 © 1980 American Chemical Society